Comparative Evaluation of Field Oriented Control and Direct Torque Control Methodologies in Field Weakening Regions for Interior Permanent Magnet Machines

Hamidreza Gashtil
School of Engineering
Newcastle University
Newcastle,UK

Volker Pickert
School of Engineering
Newcastle University
Newcastle,UK

Dave Atkinson
School of Engineering
Newcastle University
Newcastle,UK

Damian Giaouris
School of Engineering
Newcastle University
Newcastle,UK

Mohamed Dahidah
School of Engineering
Newcastle University
Newcastle,UK

***Abstract*—The comparative study on the field-oriented control (FOC) and direct-torque control (DTC) algorithms for interior permanent magnet (IPM) machine is presented in this paper. The study covers the dynamic performance of IPM under these two control strategies in constant torque and field weakening (FW) regions. The analyzation of power switches losses including the switching and conduction loss also are discussed as IPM is controlled with applying the aforementioned control strategies. So far, the critical evaluation on the basis of the power electronic losses and dynamic performance of IPM in all operational regions has not been presented. In this paper, the analytical and simulation results are provided in order to demonstrate the advantages and disadvantages of each control methodology.**

Keywords— Permanent magnet machines, field weakening, switching loss, conduction loss, direct torque control, field oriented control

I. INTRODUCTION

Nowadays, the permanent magnet motors are widely used in traction applications due to having high power density and low motor volume [1]. These features are resulted from the absence of field winding inside the rotor as the rotor flux is produced with helping of the placed permanent magnet materials in rotor structure. As the reluctance torque for IPM machines in FW regions forming the effective part of the electromagnetic torque, the PM motors achieve the wide constant power operational range which is suitable for many applications[2].

The high-performance control strategies needs to be applied in order to extract the merit performance of PM machines [3]. These control strategies provide the optimal controls such as maximum torque per ampere and FW [4]. The DTC and FOC are two high-performance control strategies which able to achieve the optimal performance with effectively controlling the motor torque and flux [5].

In DTC, the stator voltage vectors is directly selected based on the comparison results of the motor torque and motor flux with their reference values [6]. This type of selection of stator voltage vector causes that the PWM signal generator does not require. This introduce the concept of variable switching frequency performance which are improved with helping of space vector modulation [7]. In [8], the current controllers and position feedback are used in DTC for estimating torque and flux. The applied current controllers and position sensor introduce delay and extra cost respectively in the system. Therefore, the proposed DTC in [6] removes the applied current controllers in conventional DTC and uses the position sensor just for initialization. As the estimated flux in low motor speed operation is always a concern for DTC, the sophisticated flux estimator is presented in [9].

The mentioned contributions for DTC improve the performance of the control strategy, but they add the complexity to the scheme. In FOC, However in FOC strategy, the current controllers plays the main roles to control of rotor flux and torque of the electric motors. The outputs of these controllers shape the reference voltage vector which is produced by applying the power switches gate signal resulted of PWM signal generator. Therefore, the control platform based on fix switching frequency scheme is provided in FOC. Furthermore, the better control performance in low speed operation is achieved in FOC as the resulted of controlling the rotor flux in d-axis of current controller without implementing any stator flux estimator [10].

There are some researches on comparison of DTC and FOC based on the implementation complexity for the control scheme, dynamic performance and parameter sensitivity. However, the comparison analyzation of dynamic performance for DTC and FOC in high speed operational regions such as first stage of FW (FWI) and second stage of FW (FWII) has not been address. Furthermore, the comparison loss analyzation for power electronics devices has not been presented for the IPM controlled by DTC and FOC. This researches focuses on filling the aforementioned gaps to provide the wider vision of comparison for DTC and FOC.

The paper is organized as follow. Section II explains the structure of FOC for IPM and provides the mathematic loss model for power electronics devices. The description of the proposed DTC is presented in Section III. Section IV provides the comparison simulation results of dynamic responses of applied DTC and FOC in the constant torque, FWI and FWII operational regions. This section also illustrates the simulation results for conduction and switching losses for IGBT based conventional three phase inverter. Finally, the work is concluded in Section IV.

II. CONTRO STRATEGIES AND LOSS MODELS OF POWER ELECTRONICS DEVICES

A. FOC for IPM Machine in CT,FWI and FWII Regions

Controlling the flux producing current i_{ds}^e and torque producing current i_{qs}^e plays the key role in FOC strategies. In rotor based FOC, the d-axis of the synchronous frame is aligned to the position of the permanent magnet rotor flux φ_m. Therefore, the dynamic equations of the IPM machine in synchronous frame can be defined by using the d-q axis of stator voltages V_{dqs}^e as follow:

$$\frac{d}{dt}\begin{bmatrix} i_{ds}^e \\ i_{qs}^e \end{bmatrix} = \begin{bmatrix} \frac{-r_s}{L_d} & w_e\frac{L_q}{L_d} \\ -w_e\frac{L_d}{L_q} & \frac{-r_s}{L_q} \end{bmatrix}\begin{bmatrix} i_{ds}^e \\ i_{qs}^e \end{bmatrix} - \frac{w_e\varphi_m}{L_q}\begin{bmatrix} 0 \\ 1 \end{bmatrix} + \begin{bmatrix} \frac{V_{ds}^e}{L_d} \\ \frac{V_{qs}^e}{L_q} \end{bmatrix} \quad (1)$$

In (1), the electrical speed is presented by w_e and L_s, L_q are the direct and quadrature axis stator inductances which form the effective part of stator flux as follow:

$$\lambda_{ds}^e = L_d i_{ds}^e + \varphi_m, \quad \lambda_{qs}^e = L_q i_{qs}^e \quad (2)$$

Based on the λ_{dqs}^e and i_{dqs}^e the electromagnetic torque can be generated in IPM machine by:

$$T_e = \frac{3P}{4}\left(\lambda_{dq}^e \times i_{dqs}^e\right) = \frac{3P}{4}\begin{vmatrix} \vec{i} & \vec{j} & \vec{k} \\ \lambda_{ds}^e & \lambda_{qs}^e & 0 \\ i_{ds}^e & i_{qs}^e & 0 \end{vmatrix}$$
$$= \frac{3P}{4}\left[\varphi_m i_q^e + \left(L_d - L_q\right) i_{ds}^e i_{qs}^e\right] \quad (3)$$

The stator current vector $\overrightarrow{i_{dqs}^e}$ in IPM machines is limited with respect to the capacity of motor and inverter currents. In this paper, the maximum available current is defined by I_s. As $\overrightarrow{i_{dqs}^e} = i_{ds}^e + j i_{qs}^e$, the reference d-q axis currents i_{dqs}^{e*} effect on the position of $\overrightarrow{i_{dqs}^e}$ and different torque can be produced by machine.

The maximum torque per ampere (MTPA) is generated in IPM machine when the angle of $\overrightarrow{i_{dqs}^e}$ placed in:

$$\beta = \sin^{-1}\left[\frac{-\varphi_m + \sqrt{\varphi_m{}^2 + 8(L_q - L_d)^2 I_s^2}}{4(L_q - L_d) I_s}\right] \quad (4)$$

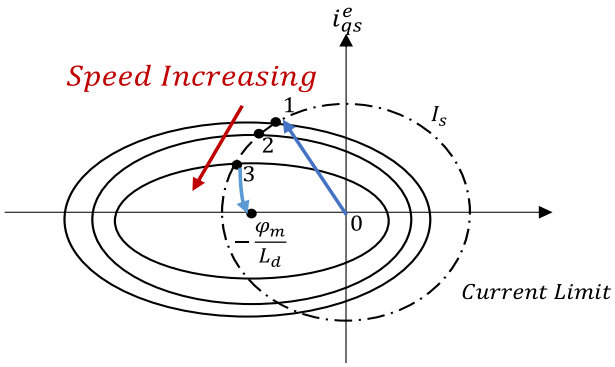

Fig. 1 Current and Voltage constraint for IPM machine

Therefore, applying the d-q axis reference current which satisfy the current limitation and (4) is main target in order to obtain the MTPA. As shown in Point 1 in Fig. 1, by keeping the applied reference current based on the MTPA concept, the motor operate in constant torque region. As the speed reaches to the base speed, the maximum voltage V_s is provided by the inverter. To provide the maximum power operation, the voltage needs to be kept in its maximum. Therefore, this could be achieved by reducing the flux which is controlled by i_{ds}^e as derived in (2). This flux reduction is called the FWI and the constant power can be produced as both current and voltage constraints are satisfied (Points 1 to 3 in Fig. 1). In FWI, the new reference currents needs to be applied to satisfy both conditions as follow:

$$\frac{i_q^{e2}}{(V_s)^2/(w_e L_q)^2} + \frac{(i_d^e - \frac{\varphi_m}{L_d})^2}{(V_s)^2/(w_e L_d)^2} \le 1 \quad (5)$$

$$(i_d^e)^2 + (i_q^e)^2 \le (I_s)^2 \quad (6)$$

The approach which has been considered in this paper for designing the reference current for FWI is applying the maximum available of $i_q^e = \sqrt{(I_s)^2 - (i_d^{e*})^2}$ in (6) and substitute it in (5) to calculate i_d^{e*}. As the speed further increases (Point 3 to $-\frac{\varphi_m}{L_d}$ in Fig. 1), the parts of (1) contained of w_e have the most impact to extract the stator voltage. So, the voltage equation can be simplified as follow:

$$(L_d i_q^e)^2 + (L_d i_d^e + \varphi_m)^2 = (\frac{V_s}{w_e})^2 \quad (7)$$

In this operational region (FWII), the current constraint cannot be satisfied anymore and the maximum torque per flux scheme needs to be considered to calculate the reference currents. This could be achieved by substituting (2) in (7) and rewrite i_{ds}^e and i_{qs}^e it in terms of λ_{ds}^e. Then, the new form of (3) based on the λ_{ds}^e as follow:

$$T_e^2 = \left(\frac{3P}{4}\right)^2 \left(\lambda_d - L_q\frac{\lambda_d - \varphi_m}{L_d}\right)^2 \left(\frac{(\frac{V_s}{w_e})^2 - \lambda_d{}^2}{L_q^2}\right) \quad (8)$$

Therefore, the reference flux λ_{ds}^{e*} which produces the maximum torque in IPM machine can be achieved. Based on

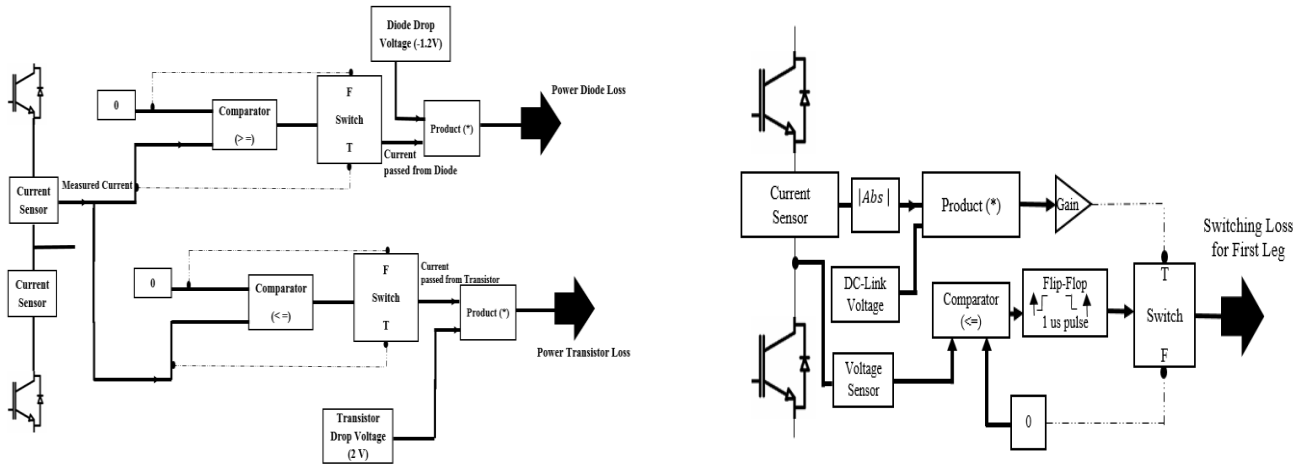

Fig. 2 Loss in power electronic devices (a) conduction loss (b) switching loss

the calculatedλ_{ds}^{e*}, the reference currents can be achieved for FWII as follow:

$$i_d^{e*} = \frac{\lambda_d - \varphi_m}{L_d} \tag{9}$$

$$i_q^{e*} = \frac{(\frac{V_s}{W_e})^2 - \lambda_d^{\,2}}{L_q^2} \tag{10}$$

B. Simplified Loss Model for Power Electronic Devices

The conduction and switching losses are two mains loss for power electronic devices [11]. The conduction loss of the IGBT modules has been divided to the loss of the switch and loss of the inverse diode. As shown in Fig.2 (a), the collector to emitter voltage (V_{CE}) is multiplied to passing current of the switch to calculate the conduction loss of the switches. As the freewheeling current in each leg passes from the inverse diode, therefore the diode conduction loss can be calculated based on its forward voltage and passed current. It should be noticed that the conduction drop voltage of the power switches and forward diode voltage can be found the datasheet of the power switches.

To determining the switching loss of the power devices, a short pulse of 1 micro second is produced in each switching event. In this time pulse duration T_{pulse}, the current passed from the power switch and the value of the DC-link voltage plays the main role for switching power loss calculation. The value of the Gain block shown in Fig. 2b depends on the total switching loss E_{on+off}, which is mentioned in datasheet of the power device and it depends on the applied collector voltage V_{CC} and current I_{CC}. So, the value of the Gain can be defined as follow:

$$Gain = \frac{E_{on+off}}{(T_{pulse} V_{CC} I_{CC})} \tag{11}$$

As shown in Fig. 2b, the flip-flop block which could be triggered on raising edge (for switching loss in turn-on event) and falling edge (for switching loss in turn-on event). The low pass filter is also placed in output of the switching loss calculation to provide the average switching loss. The power electronic devices used in this paper is SEMiX603GB066HDs.

III. PROPOSED DTC FOR IPM IN CT, FWI AND FWII REGIONS

In proposed DTC strategy, the stator flux and torque of the machine are directly controlled by an optimal voltage switching look-up table. To produce the reference torque signal, the d-q axis currents explained in section two are used depends on the operational region. These reference current are also used to produce stator flux in synchronous frame, explained in (2), and then the magnitude of reference stator flux in stationary frame λ_{dqs}^{s*} is achieved by:

$$|\lambda_{dqs}^{e*}| = |\lambda_{dqs}^{s*}| \tag{12}$$

By defining the reference torque and stator flux with helping of i_{dqs}^{e*} the look-up table for these reference signals are not required any more. To estimate the λ_{dqs}^{s}, the voltage equation of the IPM machine in stationary is used and the low pass filter LPC substitute in place of the integration term which always introduce the drift problems.

$$\lambda_{dqs}^{s} = \frac{T_c(V_{dqs}^{s} - r_s i_{dqs}^{s}) + \varphi_m e^{j\theta}}{T_c s + 1} \tag{13}$$

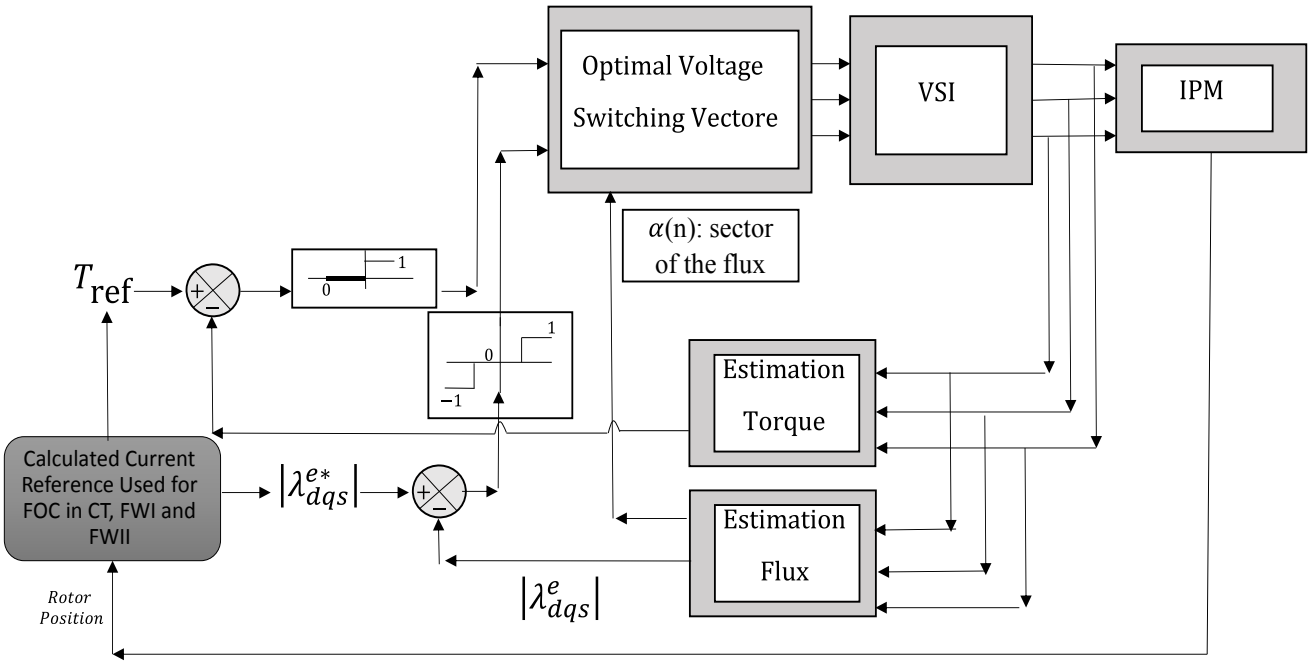

Fig. 3 Proposed DTC where the reference torque and flux are achieved based on the calculated current for FOC

The inverse of T_c present the corner frequency of the LPC. Then, the estimated flux λ^s_{dqs} is used for producing the torque estimation with helping (3). The currents used in torque estimations needs also be in stationary frame. As shown in Fig. 3, the two level and three level hysteresis controllers are used for controlling the torque and flux respectively. The outputs of these two hysteresis controller are used to apply the suitable stator voltage vector to IPM machine. The applied voltage vector satisfies the required increment or decrement in torque and flux. If the estimated torque value of the induction machine was lower than the desired value, then the torque of the machine needs to be raised by applying the voltage vector which increasing the flux level in the same direction of the machine speed and vice versa. As sown in Fig. 3, the position of the stator flux is used to determine the voltage vector.

IV. SIMULATION RESULTS

To analyses the performance of the DTC and FOC, the IPM motor with specifications mentioned in Table. 1 is modeled in Matlab Simulation. The calculated reference currents i^{e*}_{dqs} , explained in section II, are applied to IPM machine and results are presented in Fig. 4. As shown in Fig. 4a, the flux producing current and torque producing current are followed by their reference signals. In CT region, the both currents are constant which causes the motor generates the constant torque. The motor continues to operate in this region till the speed reaches to the base value (2500 RPM in Fig. 4, 5 b). As shown in Fig. 5a, the motor controlled with DTC strategy in CT region has the constant reference flux and torque which are followed by the motor flux and torque. However as shown in Fig. 5a2, in very slow speed operation, the torque contained of oscillations before tracking the reference torque signal. Comparing of Fig. 4b and Fig. 5b shows that the torque ripple in all operational regions for DTC is less than FOC. This ripples in FOC are the results of the current controller's performances. The dynamic performance of the current regulators could be improved by applying the accurate tuning methods or increasing the switching frequency that reduce the motor currents ripples. In this FOC applied to IPM motor, the switching frequency is constant and has the value of 10 KHz. However in the implemented DTC, the fix switching frequency has not been considered. Therefore, the gate signals of the power switches can be updated much faster that 10 KHz which is the case for FOC. This causes that the motor torque in DTC has lower ripples comparing with FOC and the switching loss in DTC is more than FOC (Fig. 4-5b,c). The conduction loss is almost the same for DTC and FOC strategies. The small difference between Fig. 4d and Fig. 5d is the result of the stator currents ripples which are effected by the switching frequency. Higher switching frequency causes the lower current ripples which leads to lower conduction loss.

As shown in Fig. 4a in FWI region, i^{e*}_{ds} and i^{e*}_{qs} are reduced to satisfy the current and voltage constrains explained in Fig. 1. In this region, the maximum power is provided by the IPM machine. This is the true scenario for DTC strategy which tries to reduce the flux that allows to IPM machine for operating in higher speed (Fig. 5a). In FWII region where the current constraint cannot be satisfied any more, then the i^{e*}_{ds} shrinks inside the current limitation and its value increases (Fig. 4a). It should be noticed that the magnitude of reference stator flux in DTC is also reduced in FWII based on (2).

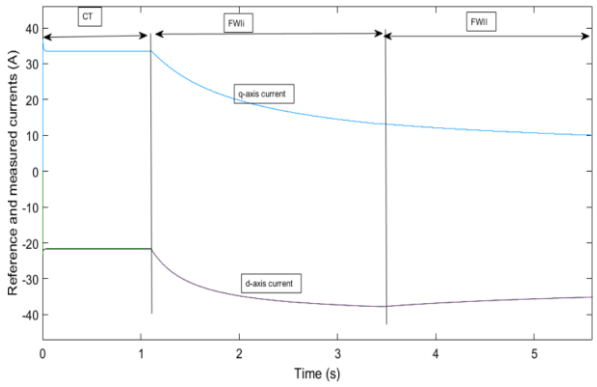

(a)

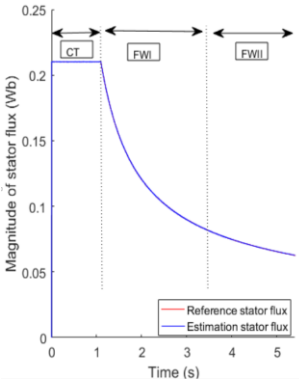

(b1)

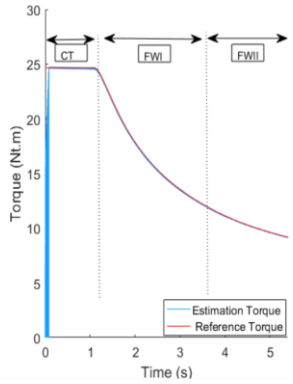

(b2)

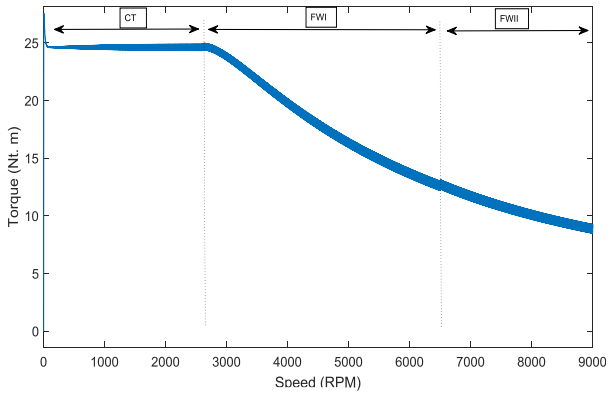

(b)

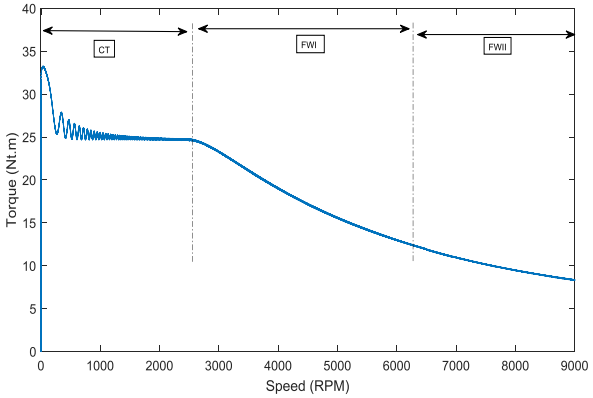

(b)

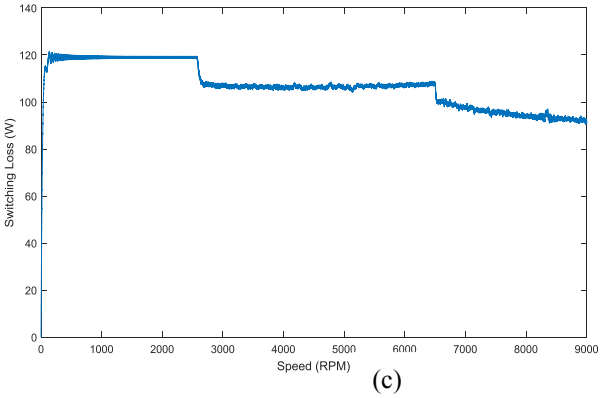

(c)

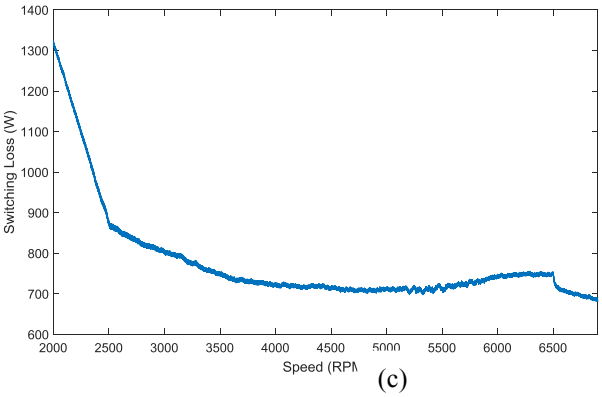

(c)

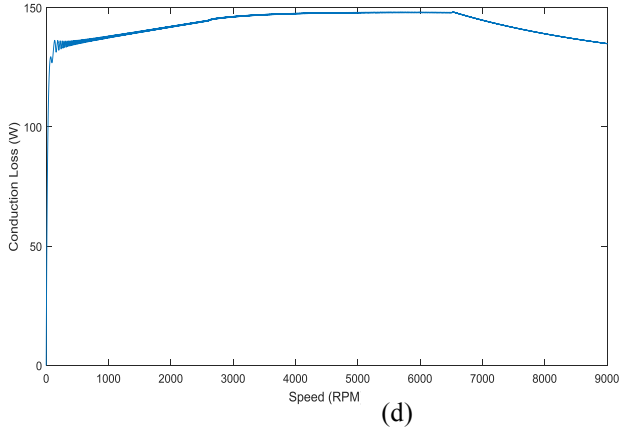

(d)

FOC results for IPM (a) Reference-responds motor currents (b) Torque (c) Switching loss (d) Conduction loss

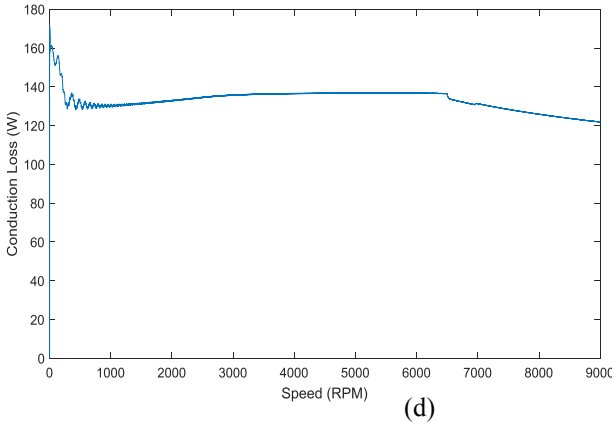

(d)

DTC results for IPM (a) Reference-responds motor currents (b) Torque (c) Switching loss (d) Conduction loss

V. CONCLUSION

This paper present the comparative evaluation between DTC and FOC strategies for IPM machine in CT, FWI and FWII regions. The smoother electromagnetic torque is generated with DTC which is not limited with constant switching frequency of 10 KHz which is the case for FOC strategy in this paper. As the results of the fix gate signals switching, the lower switching loss is achieved with controlling IPM based on the FOC method. However, the conduction loss is reduced with applying the DTC method to IPM machine operating in high speed regions.

Appendix

Table. 1 IPM specifications

DC-Link Voltage	300 V	Power (rated)	8.8 KW
Inductance (L_d)	3.05 mH	Base speed	2600 rpm
Inductance (q)	6.2 mH	Current	40 A
Number of Poles	6	φ_m	.094 Wb

Reference

[1] K. H. Nam, *AC Motor Control and Electrical Vehicle Applications*: Taylor & Francis, 2010.

[2] H. Gashtil, M. Kimabeigi, J. Goss, and S. Roggia, "Modelling an Interior Permanent Magnet Traction Motor Based on Current Signals Produced in a Space Vector Modulation," in *2018 XIII International Conference on Electrical Machines (ICEM)*, 2018, pp. 833-839.

[3] H. Le-Huy, "Comparison of field-oriented control and direct torque control for induction motor drives," in *Industry Applications Conference, 1999. Thirty-Fourth IAS Annual Meeting. Conference Record of the 1999 IEEE*, 1999, pp. 1245-1252.

[4] Y. Inoue, S. Morimoto, and M. Sanada, "Comparative study of PMSM drive systems based on current control and direct torque control in flux-weakening control region," *IEEE Transactions on Industry Applications,* vol. 48, pp. 2382-2389, 2012.

[5] F. Niu, B. Wang, A. S. Babel, K. Li, and E. G. Strangas, "Comparative evaluation of direct torque control strategies for permanent magnet synchronous machines," *IEEE Transactions on Power Electronics,* vol. 31, pp. 1408-1424, 2016.

[6] M. F. Rahman, L. Zhong, and K. W. Lim, "A direct torque-controlled interior permanent magnet synchronous motor drive incorporating field weakening," *IEEE Transactions on Industry Applications,* vol. 34, pp. 1246-1253, 1998.

[7] T. G. Habetler, F. Profumo, M. Pastorelli, and L. M. Tolbert, "Direct torque control of induction machines using space vector modulation," *IEEE Transactions on Industry Applications,* vol. 28, pp. 1045-1053, 1992.

[8] C. French and P. Acarnley, "Direct torque control of permanent magnet drives," *IEEE Transactions on Industry Applications,* vol. 32, pp. 1080-1088, 1996.

[9] K. D. Hurst, T. G. Habetler, G. Griva, and F. Profumo, "Zero-speed Tacholess IM Torque Control: Simply a Matter of Stator Voltage Induction," *IEEE Transaction on Industry application,* vol. 34, 1995.

[10] D. Casadei, F. Profumo, G. Serra, and A. Tani, "FOC and DTC: two viable schemes for induction motors torque control," *IEEE transactions on Power Electronics,* vol. 17, pp. 779-787, 2002.

[11] M. Mirjafari and R. S. Balog, "Survey of modelling techniques used in optimisation of power electronic components," *IET Power Electronics,* vol. 7, pp. 1192-1203, 2014.